1	Benthic Anaerobic Respiration Enhances Bottom-water Acidification in the northern Guif
2	of Mexico
3	
4	Hongjie Wang ¹ , John Lehrter ² , Kanchan Maiti ³ , Katja Fennel ⁴ , Arnaud Laurent ⁴ , Nancy
5	Rabalais ³ , Najid Hussain ¹ , Qian Li ¹ , Baoshan Chen ¹ , K. Michael Scaboo ¹ and Wei-Jun Cai ^{1,*}
6	1. School of Marine Science and Policy, University of Delaware, Newark, Delaware 19716
7	USA.
8	2. Department of Marine Sciences, University of South Alabama, and Dauphin Island Sea
9	Lab, Dauphin Island, Alabama 36528, USA
10	3. Department of Oceanography and Coastal Sciences, Louisiana State University, Baton
11	Rouge, Louisiana 70803, USA
12	4. Department of Oceanography, Dalhousie University, Halifax, Nova Scotia, B3H 4R2,
13	Canada
14	
15	Submitted to Geophysical Research Letters
16	*Corresponding to Dr. Wei-Jun Cai (wcai@udel.edu)
17	
18	Key points
19	1. The observed pH and Ω in hypoxic bottom water are less than the <u>predicted estimated</u> values
20	from anthropogenic CO ₂ intrusion and aerobic respiration in northern Gulf of Mexico;
21	2. The additional pH and Ω declines in hypoxic water of northern Gulf of Mexico are caused by
22	sedimentbenthic anaerobic respiration, and are positively correlated to eorrelated to modeled
23	time-integrated-hypoxic area.
24	-
25	3. The additional pH and Ω decline in hypoxic water is caused by sediment anaerobic respiration
26	
27	Abstract
28	In coastal oceans affected by nutrient delivery from the land, surface water eutrophication
29	enhances ocean acidification in bottom waters. Based on an eleventen-year collection of summer
30	data from the northern Gulf of Mexico hypoxic zone, we show substantially lower pH (-
31	0.03 ± 0.06 , up to 0.14 up to 0.14) and aragonite saturation state Ω (-0.17 ± 0.39 , up to 0.9) in years

of extensive hypoxia than those predicted estimated from water column aerobic respiration, anthropogenic CO_2 increase, and their known additive effect. Severe hypoxic or even anoxic conditions, which correspond to longer water residence times, favor the accumulation of benthic anaerobic respiration products, leading to additional pH and Ω reductions. Our findings on aerobic and anaerobic processes that contribute acidification in bottom waters provide new insights on the sensitivity of coastal acidification to hypoxia under current and future climate and anthropogenic change scenarios.

Plain Language Summary

The ongoing decrease in seawater pH (the base 10 logarithm of the molar concentration of hydrogen ions) as a result of uptake of anthropogenic carbon dioxide (CO₂) from the atmosphere is known as ocean acidification, which can be enhanced by the water column aerobic respiration in the water column. Meanwhile, regions of coastal hypoxia (dissolved oxygen<2 mg L⁻¹) has increased in size and number during the last several decades because of water column eutrophication. In this study, we report that the bottom-water acidification is more severe in hypoxic water than predicted estimated from anthropogenic CO₂ intrusion and water column organic carbon respiration in northern Gulf of Mexico. More specifically, we found that the organic matter respiration in sediment ean further decreases the buffer capacity in hypoxic bottom waters. To our knowledge, this is the first study that uses data from multiple years and systematically examines the role of benthic fluxes on ocean acidification in eutrophic coastal bottom waters. The finding has significant implications for similar coastal systems that where the eutrophication-induced bottom ocean acidification is likely more severe than we thought.

1. Introduction

Ocean deoxygenation and ocean acidification (OA) resulting from natural and anthropogenic activities, are threatening marine ecosystem health (Doney, 2010; Gruber, 2011). Global warming decreases oxygen solubility and increases stratification, and thus is likely to further increase low-oxygen areas (Breitburg et al., 2018; Brewer & Peltzer, 2016). Biogeochemical models for the northern Gulf of Mexico predict that the hypoxia area (dissolved oxygen, or DO<62.5 μ mol L⁻¹) will increase by 26% between 2005-2010 and ~2100 (Laurent et al., 2018) and that the duration of hypoxia that occurs over an annual cycle will increase (Lehrter et al.,

2017). At the same time, increasing nutrient runoff is triggering eutrophication, which enhances both inorganic carbon removal in surface water, and production of more organic carbon in the water column (Smith, 2003). While eutrophication reduces surface-water acidification resulting from the anthropogenic CO₂ intrusion (Borges & Gypens, 2010; Laruelle et al., 2018; Wang et al., 2017), the respiration of organic carbon in both water column and sediment releases CO₂ back to the bottom water and accelerates bottom-water acidification (Berelson et al., 2019; Cai et al., 2011; Feely et al., 2010; Hagens et al., 2015; Wallace et al., 2014). Excess nutrient loadings have also led to the development of bottom-water hypoxic or anoxic conditions (DO=0 µmol L 1), which may further draw down local pH (pH<7.5) due to benthic flux and subsequent oxidation of reduced chemicals (Cai et al., 2017). Meanwhile, the change of riverine alkalinity and dissolved inorganic carbon input from watersheds may either increase or decrease the buffering capacity in coastal systems (Duarte et al., 2013; Salisbury et al., 2008; Van Dam & Wang, 2019). Understanding the interactions among the above processes is crucial to understanding regional coastal acidification states and impacts on ecosystem service. Eutrophication has resulted in increased accumulation of labile organic carbon in the surface sediment of the northern Gulf of Mexico (nGoM) based on the distribution of biomarkers in the sediment (Turner et al., 2004). This is likely happening in coastal oceans on a global scale (Dell'Anno et al., 2002; Turner & Rabalais, 1994; Zhao et al., 2015; Zimmerman & Canuel, 2000). As a result, Turner et al. (2008) hypothesized that benthic DO consumption has increased through time, in step with an increase in nutrient loading from the Mississippi River watershed. A coupled physical-biological model has also shown that the hypoxia formation in the nGoM is sensitive to benthic DO consumption driven by the vertical flux of organic matter from surface waters (Fennel et al., 2013). In general, the contribution of benthic DO consumption to total bottom-water DO consumption is negatively related to the hypoxic-layer depth (Fennel & Testa, 2019). For example, on average, the benthic consumption accounts for about 20~33% of the oxygen consumption in the hypoxic layer in the nGoM where the hypoxic-layer depth is only ~ 4 m above the sea bed (Fennel & Testa, 2019; Murrell & Lehrter, 2011). In comparison, the benthic consumption only contributed 3% to the total oxygen consumption in East China Sea where has a much thicker hypoxic-layer depth (~25 m). Therefore, in shallow waters and in waters where there is a pycnocline near the bottom, the bottom DO concentration is more

63

64

65

66

67

68 69

70

71

72

73

74

75

76

77

78

79

80

81

82

83

84

85

86

87

88

89

90

91

sensitive to the benthic respiration and physical processes of the bottom boundary layer (Kemp et al., 1992; Laurent et al., 2017; Yu et al., 2015).

Benthic respiration not only consumes DO and generates CO2, but also affect total alkalinity (TA) depending on the dominant redox processes at a given site, e.g., reduction of NO₃, Mn⁴⁺, Fe³⁺, and SO₄²⁻ generates TA while oxidation of NH₃, reduced Mn²⁺ and Fe²⁺, and H₂S consumes TA (Krumins et al., 2013; Van Cappellen & Wang, 1996). The ratio of benthic TA flux and DIC flux is less than 1 in shallow water (Hu & Cai, 2011), while the TA/DIC ratio in the water column is generally greater than 1.1. Therefore, benthic processes have the potential to further decrease bottom-water pH (Berelson et al., 2019), yet the observational evidence to verify this prediction has not yet been reported. Recently, Hu et al. (2017) simulated the bottom-water pH change based on two benthic DIC flux rates that were reported by Rowe et al. (2002) and a global model-derived TA/DIC of 0.25 (Krumins et al., 2013). However, benthic flux measurements in the nGoM carried out in summer 2011, under strong hypoxia, showed an average TA/DIC of 0.8 (Berelson et al., 2019). Nevertheless, Hu et al.'s (2017) simulation supports a strong implication that the bottom-water pH is sensitive to benthic anaerobic respiration products. The data from Hu et al. (2017) were collected in late July 2010, three months after the initiation of the Deepwater Horizon oil spill in mid-April, within a month after above average discharge of the Mississippi River in May and June, and shortly after tropical storm Bonnie. It is unclear whether the lowest pH values (~7.6) within the 20-m isobath close to the Louisiana-Texas border in 2010 is a recurring event or simply an isolated condition in summer 2010.

The objective of this study is to synthesize the effect of benthic processes on bottom-water pH in the nGoM from 2006 to 2017. Observations of water column carbonate chemistry, benthic fluxes, and results from a biogeochemical model are used to analyze the underlying mechanisms of any pH and Ω variability. We propose that the physical processes that support the development and maintenance of hypoxia also favor the accumulation of benthic respiration products, leading to further reductions in pH and Ω under prolonged low-oxygen concentrations.

121 2. Data and Methods

93

94

95

96

97

98 99

100

101

102

103

104

105

106

107

108

109

110

111

112

113

114

115

116

117

118

119

120

122

2.1 Seawater Carbonate Chemistry

We report the inorganic carbon data (DIC and TA) collected from 2006 to 2017 on summer cruises (Fig. \$1, Table S1), when hypoxia occurs on the Louisiana shelf. pH and DO data from 2006-2010, and 2017 have been published in prior studies (Cai et al., 2011; Hu et al., 2017; Jiang et al., 2019). DIC data that were used to calculate pH and Ω from 2011 to 2016 were published in Wang et al. (2018).



Fig. 1. The sampling locations in June, July, August, and September from 2006 to 2017 in the northern Gulf of Mexico. Upward-pointing and downward-pointing triangles represent the stations with sediment incubation in August 2016, and July 2017, respectively. Color map shows the sampling locations in different years as in Maintext (from 2006 to 2017). The grey contour or the shaded area shows the frequency of summer bottom-water hypoxia. Date source: N. Rabalais.

Briefly, Details of routine sampling and analytical methods are given in SL water samples were taken from Niskin bottles into 250-mL borosilicate glass bottles and were poisoned with 100 μL saturated HgCl₂. The samples were kept at 4°C until being analyzed in the laboratory. DIC was measured with an infrared CO₂ detector-based DIC analyzer (AS-C3 Apollo Scitech). TA was measured with the open-cell Gran titration method using a temperature-controlled, semi-automated titrator (AS-ALK2 Apollo Scitech). Certified Reference Materials were analyzed for DIC and TA for quality control. The precisions for both DIC and TA are within 2 μmol kg⁻¹ (±0.1%). Spectrophotometric pH (pHspec; Liu et al. (2011)) was collected in year 2009, 2010 and 2012-2017 (Fig. 1, Table S1). We also calculated pH (pH_(TA, DIC)) and aragonite saturation state (Ω) using CO2SYS program by choosing measured DIC and TA as the input pair (van Heuven, 2011). Silicate and phosphate concentrations was assigned as 0. The coefficients for pH

145 and Ω calculation were selected as: K_1 and K_2 value from Lueker et al. (2000); K_{HF} was from 146 Dickson & Riley (1979); K_{HSO4} was from Dickson (1990) and B_T (total boron) was from 147 Uppström (1974). DO was measured by Winkler titration. Note, all the data listed in this study 148 are from the warm season (June, July, August and September). 149 To determine how pH evolves because of anthropogenic CO₂ intrusion (from 2006 to 2017) 150 and organic carbon respiration, we did simulations following the method reported in Cai et al. 151 (2011). This study used the same representative surface water conditions as in Cai et al. (2011), 152 which were collected from the July 2007 Gulf of Mexico and East Coast Carbon Cruise 153 (GOMECC-1) in the Gulf of Mexico (S = 36.3, t = 25° C, TA = $2398.1 \mu mol kg^{-1}$). For example, 154 for summer 2006, the dried air xCO₂ in 2006 was 381.9 ppm 155 (https://www.esrl.noaa.gov/gmd/ccgg/trends/), so the equilibrated pCO2 for this water mass was 156 370.2 μatm. The balanced DIC could be calculated as 2057.2 μmol kg⁻¹ by inputting the TA and 157 equilibrated pCO₂ to CO_{2sys}. Using the same method, the balanced DIC was 2071.1 µmol kg⁻¹, 158 with dry $xCO_2 = 406.5$ ppm in 2017 by assuming all other parameters constant (Cai et al., 2011). 159 Aerobic respiration adds DIC or removes TA following the Redfield ratio (DO: DIC: TA =-138: 160 106: -17) based on the anthropogenic CO₂ equilibrated water. pH@ 25 °C and Ω@ 25 °C was 161 recalculated with CO_{2svs} by choosing the new pair of DIC and TA. With the same method, the 162 pH-DO and Ω-DO evolutions were also simulated for each sampling year, pre-industrial era and 163 year of 2100. When considering the benthic impact on bottom pH or Ω , we added benthic DO, 164 DIC and TA flux on basis of water column DO, DIC and TA concentration. Eventually, another 165 set of pH@ 25 °C and Ω@25°C can been recalculated with CO2sys.

2.2 Benthic Flux Incubation

166 167

168

169

170

171

172

173

174

175

Sediment-water exchange rates of DO, DIC and TA were observed at five stations in August 2016 and July 2017 (Fig. §1). At each station, sediments were collected using either a multicorer or a 0.25-m² box corer that was subsampled in triplicate with Plexiglas cylindrical chambers (10-cm ID x 40 cm). The overlying water column inside the core incubations collected via multicorer were adjusted to a constant height of 25 cm using custom design lids that can be positioned at any height inside the core tube. For samples collected by box corer, the cores tubes were manually inserted into the box corer sample. Immediately after collection, three incubation cores per station were immersed in a temperature-controlled recirculating water bath incubator

adjusted to the recorded bottom-water temperature. Each core was carefully filled with bottom water with minimum disturbance to the sediment-water interface and closed to ensure no visible headspace or air bubbles at the top. All cores were attached to a reservoir containing bottom water for gravity driven replenishment of water inside the cores during sampling so as not to introduce any air bubbles. The core incubation and volumetric corrections was carried out by following the method outlined by (Ghaisas et al., 2019; Steingruber et al., 2001), where, sediment consumption alone decreased the DO inside these otherwise airtight core tubes.

All sediment incubations were carried out in the dark and lasted for 18-30 hours, depending on the final DO concentrations. Water samples in the incubation tubes were collected at regular intervals. DO was measured at each sampling point using temperature-compensated microoptodes. Samples for DIC and TA were collected in 12-ml exetainers, fixed with saturated HgCl₂ and stored at 5°C until final analysis. DIC and TA were measured with the same method as for water samples. Sediment DO consumption rates and benthic fluxes (mmol m⁻² d⁻¹) of DIC and TA were calculated by linear regression of constituent concentrations and time. Regression p-values were used to determine if flux rates were significantly different from zero (α =0.2). In cases where p was higher than 0.2, a value of zero was assigned. Benthic flux rates were corrected for water column processes by subtracting rates measured in control core tubes with only bottom water. Positive sediment benthic fluxes indicated a net flux out of the sediments to the bottom water, whereas negative fluxes indicated a net flux from the bottom water into the sediments The detail sediment sampling and incubation methods are given in SI. Note that the measured benthic DO flux at Station C6 in July 2017 only was not representative of in situ flux because the overlying water used for the incubation was collected at mid-depth instead of at the bottom. However, as TA and DIC gradients in sediment porewater develop over a much longer long-time-scale than oxygen, these sites' . benthic TA and DIC fluxes are considered to be unaltered. less likely to be disturbed.

2.3 Modelled Time-integrated Low Oxygen Area

176

177

178

179

180 181

182

183

184

185

186

187

188

189

190

191

192

193

194

195

196

197

198

199

200

201202

203

204

205

206

In order to scale benthic flux over the entire hypoxic region, we adopted the time-integrated low-oxygen area from a coupled physical-biogeochemical model that is configured for the nGoM (Laurent et al., 2018). The model is an implementation of a Regional Ocean Modeling System (Shchepetkin & McWilliams, 2005), which includes a hydrological module and a

both water column and sediment before the low DO water was abated by loss of stratification or

3. Results

3.1 Interannual Variability of Bottom-water pH and Ω

lateral advection of normoxic waters.

We compared pH calculated from DIC and TA with the measured spectrophotometric pH (pH_{spec}) from a subset of cruises and found that the calculated pH was close to the pH_{spec} (Fig. \$3522). The difference between the two methods is 0.00 ± 0.02 , which is within the uncertainty of the pH calculation (Woosley et al., 2017). Therefore, this study adopted the calculated pH and Ω to ensure the longest data record. Further, we only used data points with salinity > 32 and depth between 12 m and 50 m to achieve spatial consistency across the summer cruises (Cai et al., 2011; Hu et al., 2017).

Water column pH decreases with declining DO concentration (Fig. $\frac{1+2a}{2}$). Consistent with a previous study (Cai et al., 2011), water column pH generally followed the trends $\frac{1}{2}$ predicted estimated by anthropogenic CO₂ intrusion and aerobic respiration when DO was still relatively high (DO >150 µmol L⁻¹) (Fig. $\frac{1+2a}{2}$, detailed method to derive the $\frac{1}{2}$ prediction estimation curves is in SI). However, additional pH decline in the hypoxic condition is $\frac{1}{2}$ o.03 $\frac{1}{2}$ 0.06 (mean $\frac{1}{2}$ stidev), with a maximum up to 0.14 unit lower than the $\frac{1}{2}$ predicted estimated eurve linesvalues caused by anthropogenic CO₂ intrusion and aerobic respiration (Fig. $\frac{1}{2}$ b), in contrast to pH in higher DO conditions, which is close to the $\frac{1}{2}$ predicted estimated lines (0.00 $\frac{1}{2}$ 0.04, Fig. 1a). Ω is also positively correlated with DO but there is more curvature at low DO condition in the relationship (Fig. $\frac{1}{2}$ 2c), which is consistent with a previous study (Feely et al., 2018). Additional Ω decline in hypoxic conditions is $\frac{1}{2}$ 0.17 $\frac{1}{2}$ 0.39, with a maximum up to 0.90 unit lower than the $\frac{1}{2}$ 1 predicted estimated curve (Fig. $\frac{1}{2}$ 2d).

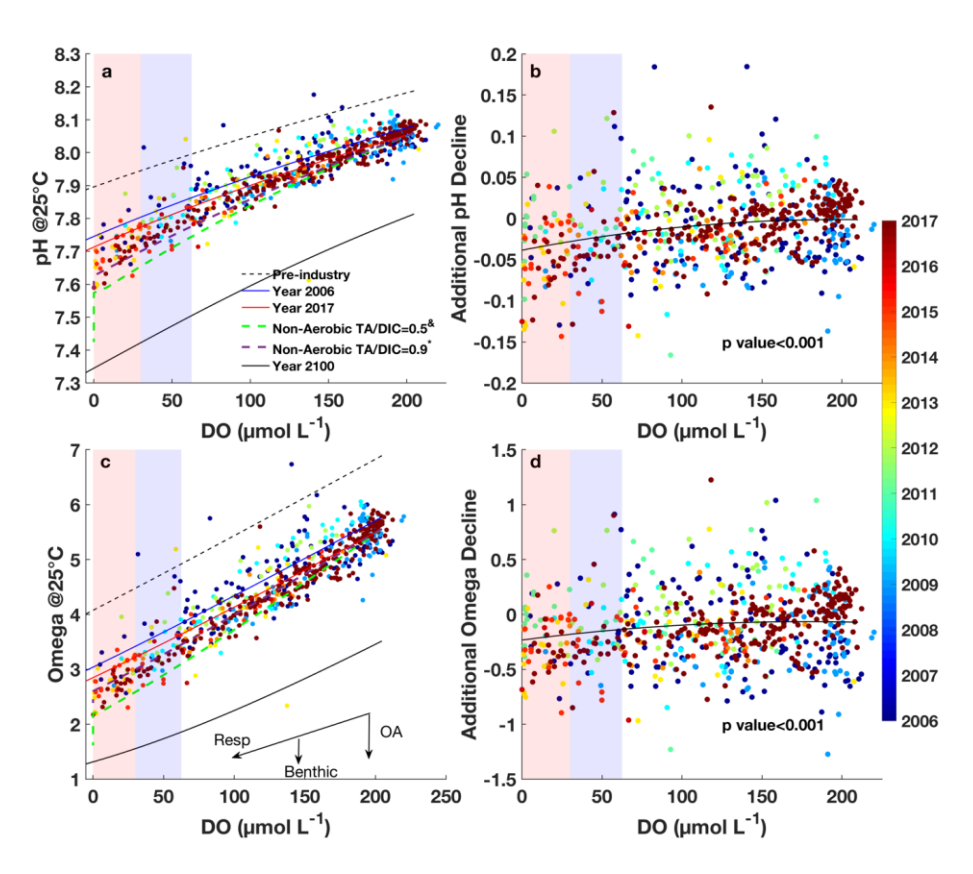


Fig. 42. (a). Relationship between pH and DO from summer 2006 to 2017 in northern Gulf of Mexico. All data presented here are with salinity > 32 and water depth between 12 m and 50 m. The black dashed, blue, red, and black solid lines represent the pH in the pre-industrial era, 2006, 2017, and 2100 with anthropogenic CO₂ intrusion and aerobic respiration. The green dashed lines represent the simulation based on our August 2016 cruise (*). The purple line denotes the simulation with results from Berelson et al. (2019)*. The method to derive the predication curve is in SI. The extensions of the green and purple dashed lines are along the zero—oxygen line (y-axis) by assuming a ten days' anoxic conditions. (b) Relation between additional pH decline and DO concentration. Note, additional pH decline is defined as the difference between measured values and predicted estimated ones from aerobic respiration of organic carbon and anthropogenic CO₂ intrusion in water column. The straight line represents the

second <u>order</u> polynomial fit. All notes are the same for panel (c, d) except they are for Ω @25°C, and all panels share the same color bar. pH and Ω changes due to increasing atmospheric CO₂, organic carbon <u>aerobic</u> respiration and benthic process are marked as OA, Resp (respiration), and Benthic in the insert panel c. The <u>patched-shaded</u> areas represent hypoxic conditions (DO<62.5 μ mol L⁻¹), while red highlights the severe hypoxic (DO<30 μ mol L⁻¹) to anoxic (DO=0 μ mol L⁻¹) conditions.

The eleven-ten years of summer pH and Ω observations (Figs. 24a, c) indicate strong year-to-year variability. The observed pH and Ω values for DO <62.5 µmol L-1 tend to be lower than the predicted_estimated_curves, for example, in summer 2017, when the largest ever recorded hypoxic area occurred (Fig. 4a2a, https://gulfhypoxia.net/research/shelfwide-cruise/?y=2017&p=press_release). Hereafter, we refer to the difference between observed pH (or Ω) and predicted_estimated pH (or Ω) caused by anthropogenic CO₂ intrusion and aerobic respiration as "additional pH decline" or "additional Ω decline." After combining all these yearly efforts, both declines were found to be significantly related to DO concentration (Figs. 4b2b, d, p<0.001).

3.2 Benthic Flux

During August 2016, the five benthic incubation stations extended from the river mouth to the open ocean (Fig. \$1, Table 1). Among them, Stations A and E were the closest and farthest station from river mouth, respectively. Station A was dominated by aerobic respiration (DO concentration was 144.7 μmol L⁻¹, Table 1). At Station E, used as a control station outside the regular hypoxic zone, bottom DO was as high as 150.3 μmol L⁻¹. Its negative TA flux indicated the dominance of aerobic respiration in sediment at this location. Station B was located at the edge of the regular hypoxic zone, while stations C and D were within the core of the hypoxic zone. Thus, we will assume hereafter that the mean DO, DIC and TA flux at Stations C and D (Table 1 and Table S2) are representative of the hypoxic zone and use those to estimate the impact of benthic respiration on bottom-water inorganic carbon system. The benthic DIC and TA flux at hypoxic station (Station C6) in July 2017 was 24.9 and 10.1 mmol m⁻² d⁻¹, respectively. Overall, the DIC/TA ratios from 2016 and 2017 fall within the ranges of other studies in the

nGoM (Table 1) and are consistent with an earlier study that found the TA/DIC flux ratio to be always less than 1 within the 100-m water depth (Hu & Cai, 2011).

3.3 Benthic Impact Simulations

DO consumption rate in the water column was not measured in August 2016, but previous shelfwide study data indicated that the average water column DO consumption is 6.8 μ mol L⁻¹ d⁻¹ (Murrell & Lehrter, 2011). At this rate, water column aerobic respiration alone should decrease bottom-water pH (or Ω) from 8.06 to 7.71 (or 5.56 to 2.86). Using the average hypoxic layer depth above the sea bed (3.9 m, Obenour et al. (2013)), the average measured DO flux from stations C and D in August 2016, and average DO consumption rate in the water column, it would take 21 days to deplete the saturated DO. The bottom-water residence time in nGoM is variable but likely longer than 30 days (Fennel & Testa, 2019; Rabouille et al., 2008). Therefore, bottom water has enough time to be impacted by benthic processes. Using the measured benthic DIC and TA flux from Station C and D in August 2016, the total DIC (or TA) production below the thermocline is 13.7 μ mol L⁻¹ d⁻¹ (or 1.6 μ mol L⁻¹ d⁻¹), leading to bottom pH and Ω under oxygen free conditions decreases to 7.57 and 2.20, respectively. In other words, with this benthic simulation, benthic respiration can further decrease bottom pH and Ω by 40% and 24% of water column aerobic respiration (Fig. 42, green dashed line).

The water column DO conditions in our shipboard incubation may not be fully representative of the *in situ* near-bottom conditions (see Method). Using an *in situ* benthic chamber technique, Berelson et al. (2019) determined that the average benthic DO, DIC and TA fluxes across the nGoM were -5.1, 41.5, and 32.4 mmol m⁻² d⁻¹ in August 2011. With this new set of fluxes, smaller pH and Ω decreases to 7.63 and 2.63, respectively, (Figs. $\frac{1}{100}$ c, purple line) are -comparable to the simulation with our own benthic data (Figs. $\frac{1}{100}$ a, c, green line).

3.4 Relationship between Bottom-water Ocean Acidification and Hypoxic Area

Both modeled hypoxic and anoxic areas vary annually (Fig. 23). The mean additional pH and Ω decline in hypoxic conditions is inversely related to the modeled time-integrated hypoxic area (r= 0.76~0.86, Fig. 2b3b). Based on the second <u>order</u> polynomial fitting between time-integrated hypoxic area and additional pH decline, the time-integrated hypoxic area should be less than $1,163\times10^3$ km² to maintain a zero-pH deviation. The annual mean additional pH decline

(-0.04 \pm 0.00, Fig. 2 α 3 α 3 α 2) from 2014 to 2017 is lower than the value from 2010 to 2012 (0.00 \pm 0.01), which is related to a greater modelled time-integrative hypoxic and anoxic area from 2014 to 2017. Similarly, the annual mean additional Ω decline from 2014 to 2017 was -0.24 \pm 0.03, which is more negative than the values from 2010 to 2012 (-0.06 \pm 0.10).

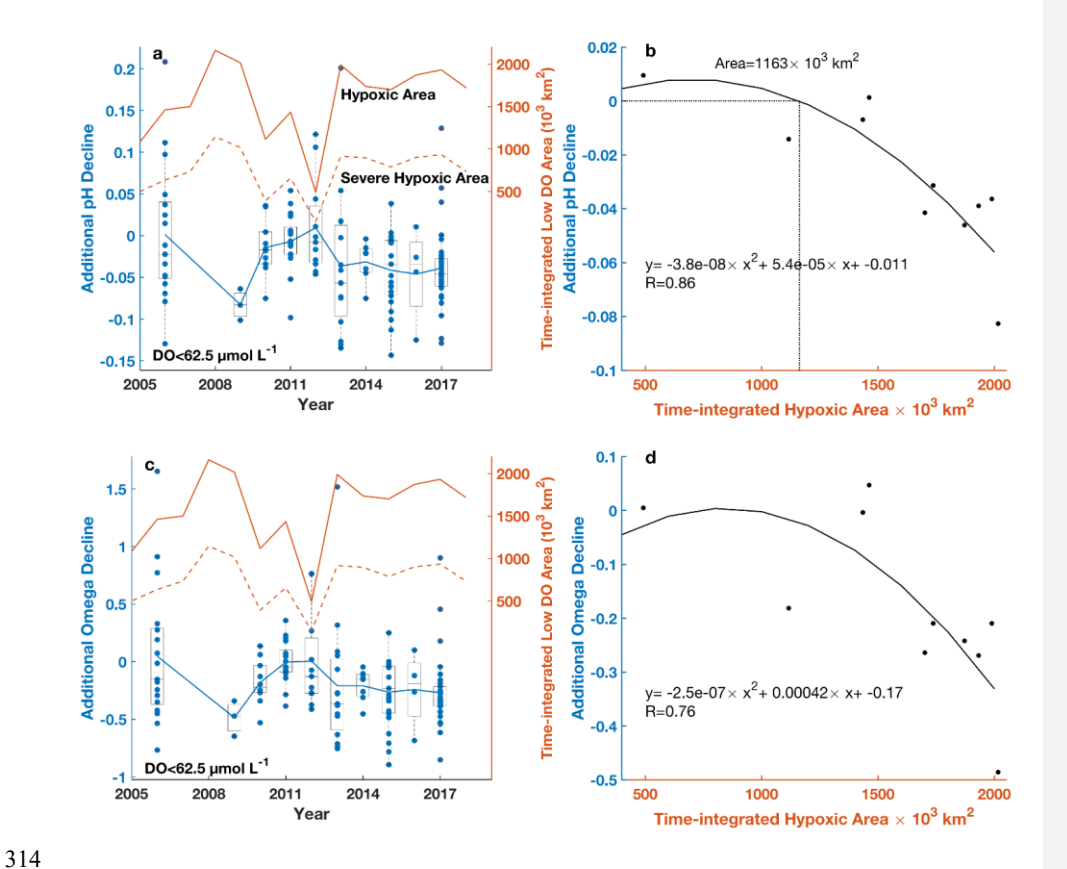


Fig. 23. (a) Distribution of observed additional pH decline at DO<62.5 μ mol L⁻¹ condition (blue points), modelled time-integrated hypoxic area (<62.5 μ mol L⁻¹, straight-connected orange line), and time-integrated severe hypoxic area (<30 μ mol L⁻¹, dashed orange line) over time. The light-gray boxplots show the distribution of observed additional pH decline in hypoxic water (<62.5 μ mol L⁻¹) in each year. The blue line connects the mean additional pH decline in each year. (b) relationship between mean additional pH decline at DO<62.5 μ mol L⁻¹ and modelled

time-integrated hypoxic area. The inserted text shows the best-fit second <u>order</u> polynomial equation. All notes in (c, d) are the same as panel (a, b) except they are for additional Ω decline. Note, additional pH or Ω decline means the difference between measured values and <u>predicted</u> <u>estimated</u> values from organic carbon respiration and anthropogenic CO_2 intrusion in water column.

326327

321

322

323

324

325

328

329

330

331

332

333

334

335

336

337

338339

340

341

342

343

344

345

346

347

348

349

350

351

4. Discussion

4.1 Benthic Processes Affecting Bottom-water pH and Ω

Benthic fluxes of DO, DIC and TA are a net result of aerobic and anaerobic processes, which are not homogeneously distributed in the nGoM. Among them, the benthic DO flux rate covaries strongly with bottom-water DO concentration with rates approaching zero when the overlying DO is depleted (Cai & Sayles, 1996; Lehrter et al., 2012; Morse & Eldridge, 2007; Nunnally et al., 2013; Rowe et al., 2002). Under DO-rich conditions, aerobic respiration dominates the benthic organic carbon respiration, which can lead to a much lower benthic TA/DIC ratio. For example, the TA and DIC flux at station B in August 2016 is 1.0 mmol m⁻² d⁻¹ and 33.3 mmol m⁻² d⁻¹, when the benthic DO flux is -24.6 mmol m⁻² d⁻¹. Aerobic respiration stops in both water column and sediment when DO is near zero. Under this condition, benthic anaerobic respiration takes over according to the early diagenetic reaction sequence, i.e., denitrification, manganese and iron reduction, and sulfate reduction. The combination of aerobic and anaerobic consumption of DO, such as denitrification, can increase the TA and DIC addition to sediment porewater at a ratio derived from the Redfield ratio (i.e., -0.16) to 0.94 with decreasing DO concentration. However, the denitrification rates are much lower compared to rates of manganese and iron reduction, which are the dominant anaerobic processes across the nGoM (Devereux et al., 2015; Devereux et al., 2019). Anaerobic respiration processes increase TA at a faster rate than DIC (Berelson et al., 2019). In addition, CaCO3 dissolution contributes to a TA:DIC ratio of 2:1. All these processes can be the reason for a higher TA/DIC ratio than aerobic respiration in sediment.

Even though the anaerobic process could increase TA in sediments, the subsequent reoxidation of the reduced species (diagenetic byproducts such as NH₄⁺ and H₂S) by O₂ should release H⁺ and eliminate the additional TA increase with a net result equivalent to the aerobic respiration (Canfield et al., 1993a). However, the two processes can be decoupled spatially and temporally forming pH maximum and minimum zones in sediment porewater (Cai et al., 2006). This can be further complicated when there is FeS and FeS₂ formation, which can be buried in sediments without readily being re-oxidized by O₂. It is possible there may be periods, such as summer, when anaerobic processes dominate, and reduced species build up in the sediments (Devereux et al., 2015). These reduced species may not be re-oxidized until fall/winter when DO is replenished (Eldridge & Morse, 2008), so there would be a period when TA is being generated, and then later being consumed. In summary, the combination of denitrification, oxidation of reduced species and iron sulfide precipitation may all be important for maintaining an observed benthic TA/DIC ratio (<1). More detail is provided in SI.

To circumvent the difficulty of not knowing exactly how much of the benthic O2 flux is caused by aerobic respiration and how much is by the re-oxidation of reduced species, we separate benthic flux into "Net-aerobic" and "Non-Aerobic" parts for the purpose to quantify the impact of benthic flux on the water column pH vs DO curve. We defined "Net-Aerobic" flux as the sum of aerobic respiration and re-oxidation of reduced species generated from anaerobic processes (Canfield et al., 1993a). The "Net-Aerobic" part of benthic respiration could be integrated with the water column aerobic respiration, because they share the same amount of DIC addition and TA removal with every mole of DO consumption (at a change ratio of 106/-17/-138). Thus, the net impact of benthic respiration on pH vs DO or Ω vs DO curve depends on the remaining fraction ("Non-Aerobic" part which includes the anaerobic respiration and CaCO3 dissolution, Table S2), which alters water column DIC and TA concentration but not DO concentration. The "Non-Aerobic" part of the TA/DIC ratio (Table S2) in August 2016 and August 2011 was 0.5, and 0.9, respectively. The lower "Non-Aerobic" TA/DIC ratio in August 2016 sediment flux led to a weaker water column buffer capacity, consequently, a higher pH reduction was predicted (Fig.2+, green line). In addition, water exchange affects the absolute time to reach hypoxia, but the pH vs DO curve remains the same as long as the water mass at the sampling location and surrounding region is impacted by the same processes (see detailed discussion in SI).

In summary, the combination of "Net-Aerobic" and "Non-Aerobic" flux can increase the benthic TA/DIC ratio from the Redfield ratio of -17/106 to a reasonably high value (<1) under a reduced DO in bottom water and near-zero DO inside the sediment. Selectively using one benthic flux under a particular DO concentration can either underestimate or overestimate the

benthic impact on bottom pH and Ω . However, the current limited sediment flux observation summarized in Table 1 is not sufficient to derive a reliable empirical equation to predict a benthic TA/DIC ratio because most of early studies did not reported benthic TA flux in the nGoM. To overcome this limitation, we did two simulations in Fig. 1-with-2 with higher and lower benthic DO flux conditions (-13.8 vs -5.1 mmol m⁻² d⁻¹). In other words, instead of exploring a single realistic scenario, our strategy was to estimate the possible ranges of benthic respiration impact on bottom-water pH and Ω (Figs. 1-22a, c). Overall, the additional pH decline caused by observed benthic DO, DIC and TA flux is smaller than the range (up to 0.2) reported by Hu et al. (2017), where a TA/DIC ratio of 0.25 derived from a global model was applied.

Laurent et al. (2018) used a coupled physical-biogeochemical model that calculated a negative additional pH decline in low-DO conditions (Figure 4b in Laurent et al., 2018), which was only attributed to the weaker buffering capacity of acidified waters because they did not have anaerobic TA flux included in the benthic parameterization. The novelty of our study is to demonstrate how the benthic anaerobic process, especially, the "Non-Aerobic" fraction impacts bottom-water OA. This is likely happening in other coastal oceans that suffer seasonal or persistent hypoxic conditions. Clearly, further study is needed to develop a more comprehensive picture of benthic respiration products under different DO condition to better refine and constrain future models of OA dynamics.

4.2 Implication for Future Coastal Bottom-water Ocean Acidification

Models by Laurent et al. (2018) predict that hypoxia in the Gulf of Mexico is likely to increase by $\sim 26\%$ by 2100 because the decreasing oxygen solubility and increasing stratification caused by climate change. This study demonstrates that as the time-integrated extent of hypoxia increases in the Gulf of Mexico, the accumulation of benthic respiration products is favored, anthropogenic CO₂ intrusion and organic carbon respiration (Fig. 34).

The increased duration of severe hypoxia and anoxia (Laurent et al., 2018; Lehrter et al., 2017) under a future scenario would further decrease bottom pH, because of the accumulation of benthic DIC and TA in bottom water (Fig. ± 2). The simulation based on August 2016 (Fig. ± 2), green dash line) indicates that an additional ten days of anoxic condition will results in further pH and Ω decrease decline from 7.57 to 7.41 $_{5}$ and 2.20 to 1.58, respectively (at DO=0, Fig.1).

This prediction shows the importance of anoxic duration on pH or Ω decrease. The exact amount of the additional pH (or Ω) declines by 2100 is difficult to predict, but the maximum pH (or Ω) decrease would be over 0.14 (or 0.90). These decreases are compounded by the expected pH (or Ω) decrease of 0.47 (or 2.2) due to water column aerobic respiration, anthropogenic CO_2 increase in the atmosphere, and their synergistic effects (Cai et al., 2011). Even though bottom-water Ω is still expected to be above 1 in the coming few decades, the dissolution threshold (Ω ~1) would occur sooner in bottom hypoxic waters than expected from the combined impact from anthropogenic CO_2 intrusion and aerobic respiration (Fig. 34).

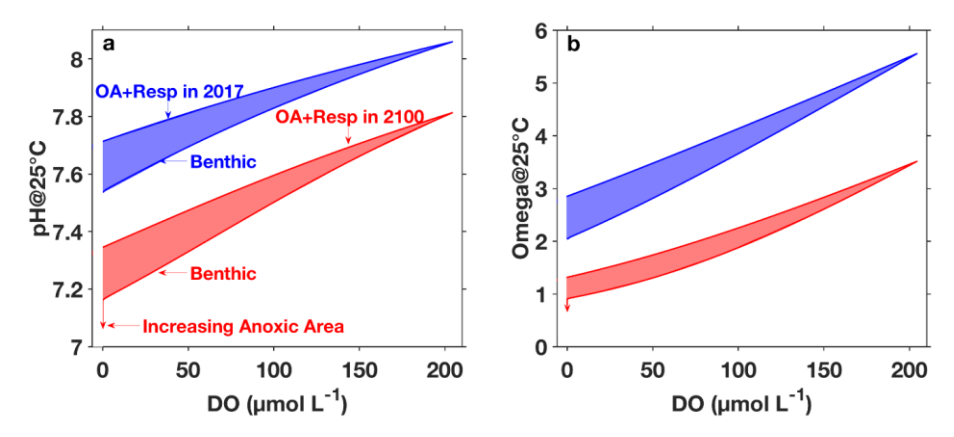


Fig. 34. Relationships between (a) pH, (b) Ω and DO in summer bottom water of the northern Gulf of Mexico. Relationships are calculated for present (year 2017, blue) and future (year 2100, red) simulations. The shades are the impact of benthic respiration on bottom pH based on August 2016 sediment dissolved oxygen, dissolved inorganic carbon, and alkalinity flux (-non-aerobic benthic TA and DIC ratio is 0.5). The vertical red arrow along DO=0 shows the impact of ten days of anoxic condition on bottom water (a) pH and (b) Ω . pH changes due to increasing atmospheric CO₂ intrusion, organic carbon respiration and observed benthic processes are marked as OA, Resp and Benthic in panel a. All notes are applicable to Ω change in panel b. Note, we used August 2016 benthic flux to simulate pH and Ω change under the future scenario.

5. Conclusion

The interannual variability of additional pH and Ω decrease is positively related to decreased bottom DO concentration. The extensive and prolonged hypoxic or anoxic conditions can

436 amplify the benthic effects on bottom pH and Ω decreases. The additional pH and Ω decrease 437 can be alleviated only if the modeled time-integrated hypoxic area appears condition is well under control (i.e., < 438 1.16×10 km² modelectime integrated hypoxicarea in the nGoMinFig.23). This is likely happening to other shallow bottom water 439 systems, such as Chesapeake Bay and Pearl River estuary. High resolution sediment profiles have confirmed a net H⁺ flux from sediment to bottom water in Long Island Sound sediments 440 441 (Fig. 7d in Zhu et al. (2006)). The benthic impact, which is known as a eutrophication legacy 442 concerning oxygen consumption, can also enhance bottom-water OA. This research adds another 443 mechanism to the big picture linking eutrophication and bottom-water OA. 444 445 6. Acknowledgement 446 We thank Xinping Hu for sharing with us the 2010-2016 data. We acknowledge the support from NSF Chemical Oceanography Program (OCE- 0752110, 1559279 and 1756815 to W-J. 447 448 Cai, OCE 1756788 to K. Maiti, OCE-1760747 to J. Lehrter, and OCE1559312 to N. Rabalais), 449 the Gulf of Mexico Research Initiative (RFP-II, GoMRI-020 to W-J. Cai and X. Hu), and NOAA Grant Nos. NA09NOS4780204 and NA16OAR4320199 (to N. Rabalais). Data from 2010 to 450 2016 are publicly available through the Gulf of Mexico Research Initiative Information and Data 451 452 Cooperative (GRIIDC) at https://data.gulfresearchinitiative.org (UDIs: R3.x164.000:0001, 453 R2.x220.000:0001, R2.x220.000:0002, R2.x220.000:0003, R2.x220.000:0004, 454 R2.x220.000:0005, R2.x220.000:0007, R2.x220.000:0008). Data archiving for 2006-2009 and 455 2017 data in Biological & Chemical Oceanography Data Management Office (BCO-DMO, 456 https://www.bco-dmo.org/search/dataset) is underway. All data in this manuscript have been 457 included as supplements for review purposes. 458 459 7. References 460 Berelson, W. M., McManus, J., Severmann, S., & Rollins, N. (2019). Benthic fluxes from 461 hypoxia-influenced Gulf of Mexico sediments: Impact on bottom water acidification, 462 Marine Chemistry, 209, 94-106. https://doi.org/10.1016/j.marchem.2019.01.004 463 Borges, A. V., & Gypens, N. (2010). Carbonate chemistry in the coastal zone responds more strongly to eutrophication than ocean acidification, Limnology and Oceanography, 55(1), 464

346-353. https://doi.org/10.4319/lo.2010.55.1.0346

- Breitburg, D., Levin, L. A., Oschlies, A., Grégoire, M., Chavez, F. P., Conley, D. J., et al.
- 467 (2018). Declining oxygen in the global ocean and coastal waters, *Science*, 359(6371).
- 468 10.1126/science.aam7240
- 469 Brewer, P. G., & Peltzer, E. T. (2016). Ocean chemistry, ocean warming, and emerging hypoxia:
- 470 Commentary, Journal of Geophysical Research: Oceans, 121(5), 365-3667.
- 471 https://doi.org/10.1002/2016JC011651
- 472 Cai, W.-J., F. Chen, E. N. Powell, S. E. Walker, K. M. Parsons-Hubbard, G. M. Staff, Y. Wang,
- 473 K. A. Ashton-Alcox, W. R. Callender, and C. E. Brett (2006), Preferential dissolution of
- carbonate shells driven by petroleum seep activity in the Gulf of Mexico, Earth and
- 475 Planetary Science Letters, 248(1-2), 227-243, http://doi.org/doi:10.1016/j.epsl.2006.05.020.
- 476 Cai, W.-J., Hu, X., Huang, W.-J., Murrell, M. C., Lehrter, J. C., Lohrenz, S. E., et al. (2011).
- 477 Acidification of subsurface coastal waters enhanced by eutrophication, *Nature Geoscience*,
- 478 4(11), 766-770. https://doi.org/10.1038/NGEO1297
- 479 Cai, W.-J., Huang, W.-J., Luther, G. W., Pierrot, D., Li, M., Testa, J., et al. (2017). Redox
- 480 reactions and weak buffering capacity lead to acidification in the Chesapeake Bay, Nature
- 481 *Communications*, 8, 369. http://doi.org/10.1038/s41467-017-00417-7
- 482 Cai, W.-J., & Sayles, F. L. (1996). Oxygen penetration depths and fluxes in marine sediments,
- 483 Marine Chemistry, 52(2), 123-131. https://doi.org/10.1016/0304-4203(95)00081-X
- 484 Canfield, D. E., Jørgensen, B. B., Fossing, H., Glud, R., Gundersen, J., Ramsing, N. B., et al.
- 485 (1993a). Pathways of organic carbon oxidation in three continental margin sediments,
- 486 Marine Geology, 113(1-2), 27-40. https://doi.org/10.1016/0025-3227(93)90147-N
- 487 Dell'Anno, A., Mei, M. L., Pusceddu, A., & Danovaro, R. (2002). Assessing the trophic state and
- 488 eutrophication of coastal marine systems: a new approach based on the biochemical
- 489 composition of sediment organic matter, Marine Pollution Bulletin, 44(7), 611-622.
- 490 https://doi.org/10.1016/S0025-326X(01)00302-2
- 491 Devereux, R., Lehrter, J. C., Beddick, D. L., Yates, D. F., & Jarvis, B. M. (2015). Manganese,
- 492 iron, and sulfur cycling in Louisiana continental shelf sediments, Continental Shelf
- 493 Research, 99, 46-56. https://doi.org/10.1016/j.csr.2015.03.008
- Dickson, A. G. (1990). Thermodynamics of the dissociation of boric acid in synthetic seawater
- from 273.15 to 318.15 K, Deep Sea Research Part A. Oceanographic Research Papers,
- 496 <u>37(5), 755-766. https://doi.org/10.1016/0198-0149(90)90004-F</u>

Field Code Changed

497	<u>Dickson, A. G., & Riley, J. P. (1979). The estimation of acid dissociation constants in sea-water</u>
498	media from potentiometric titrations with strong base. II. The dissociation of phosphoric
499	acid, Marine Chemistry, 7(2), 101-109. https://doi.org/10.1016/0304-4203(79)90002-1
500	Doney, S. C. (2010). The growing human footprint on coastal and open-ocean biogeochemistry,
501	Science, 328(5985), 1512-1516. https://doi.org/10.1126/science.1185198
502	Duarte, C. M., Hendriks, I. E., Moore, T. S., Olsen, Y. S., Steckbauer, A., Ramajo, L., et al.
503	(2013). Is ocean acidification an open-ocean syndrome? understanding anthropogenic
504	impacts on seawater pH, Estuaries and Coasts, 36(2), 221-236.
505	https://doi.org/10.1007/s12237-013-9594-3
506	Ebner, B. (2019). Spatiotemporal Variation of Benthic Silica Fluxes in the NGOM Shelf, (Master
507	thesis). Louisiana State University, # 4883.
508	https://digitalcommons.lsu.edu/gradschool_theses/4883
509	Eldridge, P. M., and J. W. Morse (2008), Origins and temporal scales of hypoxia on the
510	Louisiana shelf: Importance of benthic and sub-pycnocline water metabolism, Marine
511	Chemistry, 108(3-4), 159-171, doi:https://doi.org/10.1016/j.marchem.2007.11.009.
512	Feely, R. A., Alin, S. R., Newton, J., Sabine, C. L., Warner, M., Devol, A., et al. (2010). The
513	combined effects of ocean acidification, mixing, and respiration on pH and carbonate
514	saturation in an urbanized estuary, Estuarine, Coastal and Shelf Science, 88(4), 442-449.
515	https://doi.org/10.1016/j.ecss.2010.05.004
516	Feely, R. A., Okazaki, R. R., Cai, WJ., Bednaršek, N., Alin, S. R., Byrne, R. H., & Fassbender,
517	A. (2018). The combined effects of acidification and hypoxia on pH and aragonite saturation
518	in the coastal waters of the California current ecosystem and the northern Gulf of Mexico,
519	Continental Shelf Research, 152, 50-60. https://doi.org/10.1016/j.csr.2017.11.002
520	Fennel, K., Hetland, R., Feng, Y., & DiMarco, S. (2011). A coupled physical-biological model of
521	the Northern Gulf of Mexico shelf: model description, validation and analysis of
522	phytoplankton variability, Biogeosciences, 8(7), 1881-1899.
523	Fennel, K., Wilkin, J., Levin, J., Moisan, J., O'Reilly, J., & Haidvogel, D. (2006). Nitrogen cycling in
524	the Middle Atlantic Bight: Results from a three-dimensional model and implications for the
525	North Atlantic nitrogen budget, Global Biogeochemical Cycles, 20(3), GB3007.
526	https://doi.org/10.1029/2005GB002456
527	
1	

528 529 Gruber, N. (2011). Warming up, turning sour, losing breath: ocean biogeochemistry under global 530 change, Philosophical Transactions of the Royal Society of London A: Mathematical, 531 Physical and Engineering Sciences, 369(1943), 1980-1996. 532 https://doi.org/10.1098/rsta.2011.0003 533 Hagens, M., Slomp, C., Meysman, F., Seitaj, D., Harlay, J., Borges, A., & Middelburg, J. (2015). 534 Biogeochemical processes and buffering capacity concurrently affect acidification in a 535 seasonally hypoxic coastal marine basin, Biogeosciences, 12(5), 1561-1583. 536 https://doi.org/10.5194/bg-12-1561-2015 537 Hetland, R. D., & DiMarco, S. F. (2008). How does the character of oxygen demand control the 538 structure of hypoxia on the Texas Louisiana continental shelf?, Journal of Marine Systems, 539 70(1), 49-62. https://doi.org/10.1016/j.jmarsys.2007.03.002 540 Hu, X., Li, Q., Huang, W.-J., Chen, B., Cai, W.-J., Rabalais, N. N., & Eugene Turner, R. (2017). 541 Effects of eutrophication and benthic respiration on water column carbonate chemistry in a 542 traditional hypoxic zone in the Northern Gulf of Mexico, Marine Chemistry, 194, 33-42. 543 https://doi.org/10.1016/j.marchem.2017.04.004 544 Jiang, Z. P., Cai, W. J., Chen, B., Wang, K., Han, C., Roberts, B. J., et al. (2019). Physical and 545 biogeochemical controls on pH dynamics in the northern Gulf of Mexico during summer 546 hypoxia, Journal of Geophysical Research: Oceans (124), 5979–5998. 547 https://doi.org/10.1029/2019JC015140 548 Kemp, W. M., Sampou, P. A., Garber, J., Tuttle, J., & Boynton, W. R. (1992). Seasonal 549 depletion of oxygen from bottom waters of Chesapeake Bay: roles of benthic and planktonic 550 respiration and physical exchange processes, Marine Ecology Progress Series, 85, 137-152. 551 https://doi.org/10.3354/meps085137 552 Krumins, V., Gehlen, M., Arndt, S., Cappellen, P. V., & Regnier, P. (2013). Dissolved inorganic 553 carbon and alkalinity fluxes from coastal marine sediments: model estimates for different 554 shelf environments and sensitivity to global change, *Biogeosciences*, 10(1), 371-398. 555 https://doi.org/10.5194/bg-10-371-2013 556 Laruelle, G. G., Cai, W.-J., Hu, X., Gruber, N., Mackenzie, F. T., & Regnier, P. (2018). 557 Continental shelves as a variable but increasing global sink for atmospheric carbon dioxide,

Nature Communications, 9(1), 454. https://doi.org/10.1038/s41467-017-02738-z

- 559 Laurent, A., Fennel, K., Cai, W. J., Huang, W. J., Barbero, L., & Wanninkhof, R. (2017).
- Eutrophication-induced acidification of coastal waters in the northern Gulf of Mexico:
- Insights into origin and processes from a coupled physical-biogeochemical model,
- 562 Geophysical Research Letters, 44(2), 946-956. https://doi.org/10.1002/2016GL071881
- Laurent, A., Fennel, K., Hu, J., & Hetland, R. (2012). Simulating the effects of phosphorus
- 564 limitation in the Mississippi and Atchafalaya River plumes, *Biogeosciences*, 9(11), 4707-
- 565 4723. https://doi.org/10.5194/bg-9-4707-2012
- Lehrter, J., Beddick, D., Jr., Devereux, R., Yates, D., & Murrell, M. (2012). Sediment-water
- fluxes of dissolved inorganic carbon, O2, nutrients, and N2 from the hypoxic region of the
- Louisiana continental shelf, *Biogeochemistry*, 109(1-3), 233-252.
- 569 https://doi.org/10.1007/s10533-011-9623-x
- 570 Lehrter, J. C., Ko, D. S., Lowe, L. L., & Penta, B. (2017). Predicted effects of climate change on
- 571 northern Gulf of Mexico hypoxia, in Modeling coastal hypoxia: Numerical Simulations of
- 572 Patterns, Controls and Effects of Dissolved Oxygen Dynamics, edited by Justic, D., Rose, K.
- 573 A., Hetland, R. D. & Fennel, K., pp. 173-214, Springer International Publishing.
- Liu, X., Patsavas, M. C., & Byrne, R. H. (2011). Purification and characterization of meta-Cresol
- 575 <u>purple for spectrophotometric seawater pH measurements, Environmental Science & </u>
- 576 <u>Technology</u>, 45(11), 4862-4868. https://doi.org/10.1021/es200665d
- Lueker, T. J., Dickson, A. G., & Keeling, C. D. (2000). Ocean pCO2 calculated from dissolved
- inorganic carbon, alkalinity, and equations for K1 and K2: validation based on laboratory
- measurements of CO2 in gas and seawater at equilibrium, Marine Chemistry, 70(1), 105-
- 580 <u>119. https://doi.org/10.1016/S0304-4203(00)00022-0</u>
- 581 Morse, J. W., & Eldridge, P. M. (2007). A non-steady state diagenetic model for changes in
- sediment biogeochemistry in response to seasonally hypoxic/anoxic conditions in the "dead
- zone" of the Louisiana shelf, Marine Chemistry, 106(1), 239-255.
- 584 https://doi.org/10.1016/j.marchem.2006.02.003
- Murrell, M., & Lehrter, J. (2011). Sediment and lower water column oxygen consumption in the
- seasonally hypoxic region of the Louisiana continental shelf, Estuaries and Coasts, 34(5),
- 587 912-924. https://doi.org/10.1007/s12237-010-9351-9

```
588
       Nunnally, C. C., Rowe, G. T., Thornton, D. C., & Quigg, A. (2013). Sedimentary oxygen
589
           consumption and nutrient regeneration in the Northern Gulf of Mexico hypoxic zone,
590
           Journal of Coastal Research, 63(sp1), 84-96. https://doi.org/10.2112/SI63-008.1
591
       Obenour, D. R., Scavia, D., Rabalais, N. N., Turner, R. E., & Michalak, A. M. (2013).
592
           Retrospective analysis of midsummer hypoxic area and volume in the northern Gulf of
593
           Mexico, 1985–2011, Environmental Science & Technology, 47(17), 9808-9815.
594
           https://doi.org/10.1021/es400983g
595
       Rabouille, C., Conley, D. J., Dai, M. H., Cai, W. J., Chen, C. T. A., Lansard, B., et al. (2008).
596
           Comparison of hypoxia among four river-dominated ocean margins: The Changjiang
597
           (Yangtze), Mississippi, Pearl, and Rhône rivers, Continental Shelf Research, 28(12), 1527-
598
           1537. https://doi.org/10.1016/j.csr.2008.01.020
599
       Rowe, G. T., Kaegi, M. E. C., Morse, J. W., Boland, G. S., & Briones, E. G. E. (2002). Sediment
600
           community metabolism associated with continental shelf hypoxia, northern Gulf of Mexico,
601
           Estuaries, 25(6), 1097-1106. https://doi.org/10.1007/BF02692207
602
       Salisbury, J., Green, M., Hunt, C., & Campbell, J. (2008). Coastal acidification by rivers: a threat
603
           to shellfish?, Eos, Transactions American Geophysical Union, 89(50), 513-513.
604
           https://doi.org/10.1029/2008EO500001
605
       Shehepetkin, A. F., & McWilliams, J. C. (2005). The regional oceanic modeling system
606
           (ROMS): a split-explicit, free-surface, topography-following-coordinate oceanic model,
607
           Ocean Modelling, 9(4), 347-404. https://doi.org/10.1016/j.ocemod.2004.08.002
608
       Steingruber, S. M., Friedrich, J., Gächter, R., & Wehrli, B. (2001). Measurement of
609
           denitrification in sediments with the 15N isotope pairing technique, Applied and
610
           Environmental Microbiology, 67(9), 3771-3778. https://doi.org/10.1128/AEM.67.9.3771-
611
           3778.2001
612
613
       Turner, R. E., Milan, C. S., & Rabalais, N. N. (2004). A retrospective analysis of trace metals, C,
614
           N and diatom remnants in sediments from the Mississippi River delta shelf, Marine
615
           Pollution Bulletin, 49(7-8), 548-556. https://doi.org/10.1016/j.marpolbul.2004.03.013
616
       Turner, R. E., & Rabalais, N. N. (1994). Coastal eutrophication near the Mississippi river delta,
```

Nature, 368(6472), 619-621. https://doi.org/10.1038/368619a0

618 Turner, R. E., Rabalais, N. N., & Justic, D. (2008). Gulf of Mexico hypoxia: alternate states and 619 a legacy, Environmental Science & Technology, 42(7), 2323-2327. 620 http://doi.org/10.1021/es071617k 621 Uppström, L. R. (1974). The boron/chlorinity ratio of deep-sea water from the Pacific Ocean, 622 Deep Sea Research and Oceanographic Abstracts, 21(2), 161-162. 623 https://doi.org/10.1016/0011-7471(74)90074-6 624 Van Cappellen, P., & Wang, Y. (1996). Cycling of iron and manganese in surface sediments; a 625 general theory for the coupled transport and reaction of carbon, oxygen, nitrogen, sulfur, 626 iron, and manganese, American Journal of Science, 296(3), 197-243. 627 https://doi.org/10.2475/ajs.296.3.197 628 Van Dam, B. R., & Wang, H. (2019). Decadal-scale acidification trends in adjacent North 629 Carolina estuaries: competing role of anthropogenic CO2 and riverine alkalinity loads, 630 Frontier Marine Science, 6(136). https://doi.org/10.3389/fmars.2019.00136 631 van Heuven, S., D. Pierrot, J.W.B. Rae, E. Lewis, and D.W.R. Wallace (2011), MATLAB 632 Program Developed for CO2 System Calculations, Oak Ridge, Tennessee, doi:10.3334/CDIAC/otg.CO2SYS MATLAB v1. 633 Wallace, R. B., Baumann, H., Grear, J. S., Aller, R. C., & Gobler, C. J. (2014). Coastal ocean 634 635 acidification: The other eutrophication problem, Estuarine, Coastal and Shelf Science, 148, 636 1-13. https://doi.org/10.1016/j.ecss.2014.05.027 637 Wang, H., Hu, X., Cai, W.-J., & Sterba-Boatwright, B. (2017). Decadal fCO2 trends in global 638 ocean margins and adjacent boundary current-influenced areas, Geophysical Research 639 Letters, 44, 8962–8970. https://doi.org/10.1002/2017GL074724 640 Wang, H., Hu, X., Rabalais, N. N., & Brandes, J. (2018). Drivers of oxygen consumption in the 641 northern Gulf of Mexico hypoxic waters—a stable carbon isotope perspective, Geophysical 642 Research Letters 45, 10528-10538. https://doi.org/10.1029/2018GL078571 643 Woosley, R. J., Millero, F. J., & Takahashi, T. (2017). Internal consistency of the inorganic 644 carbon system in the Arctic Ocean, Limnology and Oceanography: Methods, 15(10), 887-645 896. https://doi.org/10.1002/lom3.10208

Yu, L., Fennel, K., Laurent, A., Murrell, M., & Lehrter, J. (2015). Numerical analysis of the

12(7), 2063-2076. https://doi.org/10.5194/bg-12-2063-2015

primary processes controlling oxygen dynamics on the Louisiana shelf, Biogeosciences,

646 647

Zhu, Q., Aller, R. C., & Fan, Y. (2006). Two-dimensional pH distributions and dynamics in
 bioturbated marine sediments, *Geochimica et Cosmochimica Acta*, 70(19), 4933-4949.
 https://doi.org/10.1016/j.gca.2006.07.033
 Zimmerman, A. R., & Canuel, E. A. (2000). A geochemical record of eutrophication and anoxia
 in Chesapeake Bay sediments: anthropogenic influence on organic matter composition,
 Marine Chemistry, 69(1), 117-137. https://doi.org/10.1016/S0304-4203(99)00100-0

Table 1. Summary of DO, DIC and TA flux from the northern Gulf of Mexico. Positive flux is defined as from sediments into the bottom water.

	Date	Depth (m)	T (°C)	S	DO (μmol L ⁻¹)	Benthic DO flux (mmol m ⁻² d ⁻¹)	Benthic DIC flux (mmol m ⁻² d ⁻¹)	Benthic TA flux (mmol m ⁻² d ⁻¹)	TA/DIC
Station A#	August 2016	19.5	29.64	31.81	144.7	-13.5±0.2	33.0±2.1	-3.3±13.2	-0.1
Station B#	August 2016	45.5	24.05	36.32	161.2	-24.6±13.8	33.3±4.2	1.0±3.6	0.03
Station C#	August 2016	35.5	25.80	35.92	132.5	-13.7±0.6	39.9±13.3	15.4±21.1	0.39 [•]
Station D#	August 2016	17.5	27.51	33.77	45.0	-13.8±0.6	26.3±6.9	3.7±9.2	0.14 [•]
Station E#	August 2016	49.5	24.43	36.08	150.3	-10.9±1.0	84.5±10.5	-15.5±27.8	-0.18
Station C6	July 2017	18.4	16.98	35.12	26.7	-	24.9	10.1	0.41
Station D5	July 2017	31.4	25.23	36.08	173.4	-	16.0	0.6	0.04
Station E6	July 2017	55.1	22.53	36.21	135.8	-	5.4	2.2	0.40
Shelf nGoM ^{\$}	July 1991	17.0~21.0	25.2~26.8		6~83	-18.4~-0.82	-	-	-
(Rowe et al, 2002)		(19.0±1.8)	(26.2±0.7)	-	(26.5±37.7)	(-9.73±7.2)			
	August 1994	12.0~25.0	27.2~28.6		0~14	-1.9~-56.4	24~55		
		(20.7±7.5)	(28.1±0.8)	-	(8±7)	(-25.0±28.2)	(39.0±15.5)	-	-
Shelf nGOM®	March 2005 to August 2007	5.0~22.0	20.0~30.0	>35	58.7~125.5	-23.9~0	7.9~21.5	-	
(Lehrter et al., 2012)	August 2007	(13.5±8.3)			(100±29)	(-10±6)	(17.2±2.4)		
Shelf nGoM*		18.0~23.0	22.6~29.2	25.2~35.8	0~160	-11.8~0	24.8~58.9	24.2~49.1	0.57~0.98
(Berelson et al., 2019)	August 2011	(21.5±2.4)	(25.7±2.7)	(32.7±5.0)	(53±73)	(-5.1±4.9)	(41.5±14.0)	(32.4±11.7)	(0.80±0.2) [●]

Note, # Ebner (2019); \$ flux data without Station 1 (see details in Rowe et al. (2002)); & There were no DIC flux measurement in

March 2005 (see details in Lehrter et al. (2012)); *Flux data from entire Gulf of Mexico shelf after excluding Station 8 (see details in

Berelson et al. (2019)); ${}^{\bullet}$ TA/DIC ratio we used to simulate benthic impact on bottom-water pH and Ω (See details in text). The

⁶⁶⁰ hypoxic stations are highlighted in bold.